SECURITY & DEFENCE QUARTERLY
https://securityanddefence.pl/

High power wireless power transfer for the future of the battlefield challenges

Mohamed Zied Chaari[1], Rashid Al-Rahimi[1], Otman Aghzout[2]

[1]chaari_zied@yahoo.fr

[1]https://orcid.org/0000-0002-8770-9420

[1]Fab-Lab, Qatar scientific club, street 669 Zone 56, 9769, AL-Mamoura, Qatar

[2]Department of Computer Science Engineering, University of Abdelmalek Essaadi, BP-2222- Mhannech II, Morocco

Abstract

A significant challenge for the military lab is to reduce the weight of a combatant's battery on the battlefield. Soldiers use electronic devices powered by wearable batteries in landings, operational combat with the enemy, and defensive exercises. Soldiers should always fully charge their wearable batteries before carrying them. The average weight of the battery is approximately 20 kilograms. During military operations, fighters have numerous electronic devices, such as night-vision goggles, headphones, LMR, navigation systems, VHF radios, and sensors. There is a high probability that fighters will lose their lives if the battery they take is uncharged or empty. Many research studies have tried to increase fighting time and maintain soldier life and links based on these devices. In this work, a wireless power transmission system with an RF microwave station and RF/DC converter circuit incorporated into a bulletproof vest will be designed. This system can harvest RF microwave energy to recharge or energize the wearable battery during a military operation. The challenge here is to develop a compact device that can capture the maximum RF strength to charge batteries carried by soldiers. The proposed device therefore considers all parameters to provide sufficient energy to power a computer at 13 watts. The strength of the RF power varies with the distance between the microwave power station Pin = 100 W and the receiver circuit.

Keywords:

Antenna, high power wireless power transfer, battlefield, RF-DC rectifier, rectenna

Article info
Received: 24 March 2022
Revised: 13 July 2022
Accepted: 1 August 2022
Available online: 2 September 2022

Citation: Chaari, M.Z., Al-Rahimi, R. and Aghzout, O. (2022) 'Wireless energy transfer for the future of battlefield challenges', Security and Defence Quarterly, 40(4), pp. 9–26.. doi: 10.35467/sdq/152548.

Introduction

Previously, the combat soldier had a few items that required batteries, possibly a short-range VHF or UHF radio telecommunication, and a night vision scope (Brewster, 2020; Niesel, 2019). Every combatant had these and a requirement to power them. They included electronic sights, laser rangefinders, mini laptops, and a communications radio. What happens when a combatant's wearable battery power level drops during combat? The response is evident in the number of military companies and laboratories working to solve this problem every year and the increasing number of scientific publications. Combat soldiers typically carry batteries for a 72-hour mission (Harper, 2015; Lafontaine, 2019; Miller, 2020). In Figure 1, we see they are concerned about reliable and timely resupply and ensuring their electronics and communications are available.

US soldiers not only carried weapons but also wearable batteries. For instance, on a 72-hour operation in Kabul and Baghdad, the average combat soldier had a sixteen-pound flak jacket, a sizeable weapon, and 40 pounds of gear, including batteries for communication, navigation, and powering monitoring devices (Collins, 2015). According to a British Ministry of Defence (MoD) study, every soldier carries around 12kg of batteries for a 36-hour patrol (Miller, 2020). According to a recent analysis by the Canadian Army, soldiers carry more than 51 AA batteries and CR123 batteries for a 24-hour guard (Thales, 2016). Battery placement has become one of the most critical considerations on today's battlefields. The requirements for electrical power have grown-up exponentially over the last few years. Portable batteries have been a particular challenge for soldiers and special forces units. They must use all these devices continuously for three nights. The military is seeking longer battery charges, faster and more possibilities for recharging, extending the overall battery life, reducing the size and weight of batteries, and improving safety (Miller, 2020) . Achieving the promised capabilities offered by these technologies is directly linked to solving the power problem. The US army studies much research and works to reduce its combat soldiers' enormous and literal burden. It held a competition in 2008 to find a 4-kilogram portable power supply that could provide 20 Watts for 96 hours (1.92 kilowatt-hours) of energy. Christopher Hurley and others developed fuel cells, smart

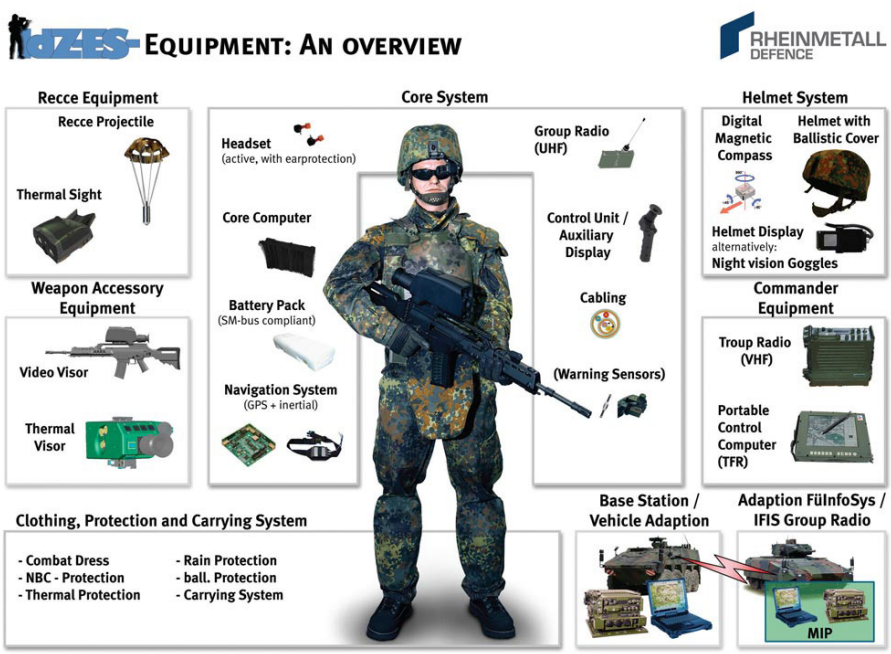

Figure 1. A fighter's equipment and batteries during a routine operation (RHEINMETALL).

grids, and environmental control units, harvesting wind and solar power and examining waste-to-energy and biofuels. He is working on more novel projects to develop a power source that converts commonly available sugars directly into electrical energy. He uses enzymes to convert sugar into energy, similar to how your body uses enzymes to convert food into energy (Sigler, 2011). Recently, the US army succeeded in implementing wireless recharge gadgets from 15 metres away (Beckhusen, 2012). In the plan, the branches' research and development centres will contribute more than six million dollars to improve wireless energy transmission efficiency over greater distances, according to a US Army announcement. Chaari *et al.* produced a study of the impact of wireless power charging on the future of battlefields (Chaari and Al-Rahimi, 2021b).

Using renewable energy sources such as solar chargers or wind power can reduce the load and weight of the batteries by providing energy. Wireless power transmission has become widely used in rescue applications because it can reduce the battery's weight during fire-fighting operations (Chaari and Al-Rahimi, 2021a; Chaari and Rahimi, 2017; Sidhu *et al.*, 2019). RF microwave energy would be sent to a small unit to wirelessly charge batteries in an electronic device (laser range finder, night vision goggles, infrared sight system, and radio system). Wireless charging solutions can reduce battery size, weight, endurance, fighting time and increase soldier strength. It consists of an RF transmitter part and a harvester circuit that uses high efficiency to harvest energy, as shown in Figure 2 and to provide electrical power to charge the wearable batteries on bulletproof vests using radiofrequency energy in the S-band (Ishibashi *et al.*, 2019; Liu *et al.*, 2020; Tran *et al.*, 2017).

There are two main subsystems in the topology design. The first subsystem studied is the RF transmitter source coupling with a higher-performance pin-fed pyramidal horn antenna. The second subsystem uses an array patch antenna to harvest RF energy associated with a rectifier circuit at a higher efficiency (Pinto *et al.*, 2021). This study looks at the possibility of energising many electronic devices by putting a soldier inside a bulletproof vest. It provides the most critical factor necessary for the soldier to perform his duties on the battlefield, namely, an approved electrical source from which to charge his battery for a 72-hour mission. This study examines the possibility of powering many electronic devices wirelessly using the harvester circuit on the bulletproof jacket, as illustrated in Figure 3. Scientists aim to reduce the weight of batteries for a 36-hour patrol to create a more intelligent battlefield. This study will examine two critical subsystems: an RF transmitter source and an RF-DC harvester. Estimating and calculating the amount of power loss in wireless power charging is necessary to determine the best antenna parameters.

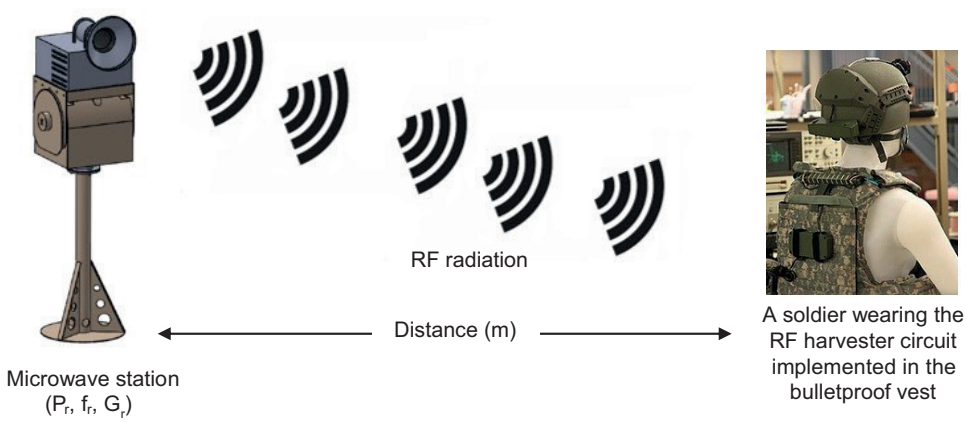

Figure 2. Illustrates the topology of a wireless energy transmission system on the battlefield.

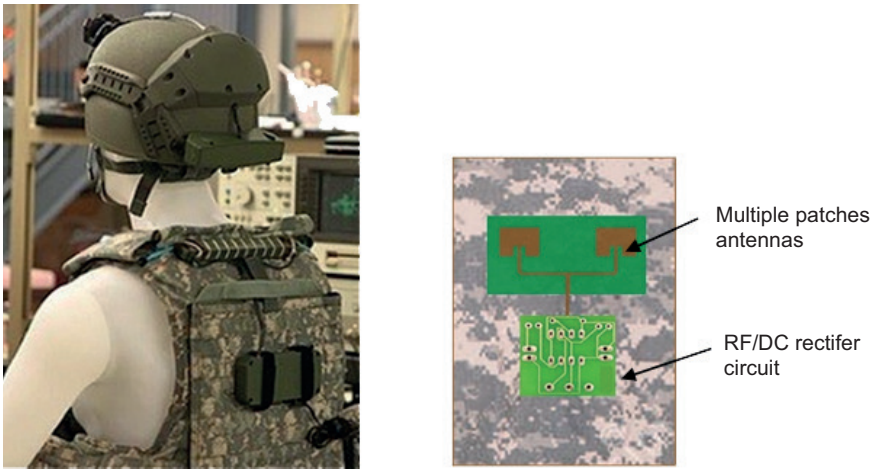

Figure 3. RF power harvesting circuit implemented on a protective vest.

Power Budget

A transmitting antenna produces a power density $W_t(\theta_t,\varphi_t)$ in the direction (θ_t,φ_t). This power density attaches to the transmitting horn antenna Gain in the given direction $G(\theta_t,\varphi_t)$, on the power of the transmitter P_t fed to it, and on the distance (D) between the transmitting point and the observation point as

$$W_t = \frac{P_t}{4\pi R^2} G_t(\theta_t,\theta_t) \tag{1}$$

The required transmitter power is calculated using the effective receiving and transmitting antennas area, as shown in Figure 4.

$$P_{rx} = P_{tx} G_{tx} G_{rx} \left(\frac{c}{4\pi D_r f_0} \right)^2 \tag{2}$$

$$P_{rx}(dB) = P_{tx} + G_{tx} + G_{rx} + 20\log 10\left(\frac{\lambda}{4\pi D_r} \right)^2 \tag{3}$$

To calculate the effective area of a patch antenna over a perfect ground plane, the following formula is used:

$$A_{er} = \frac{G_r \lambda^2}{4\pi} \tag{4}$$

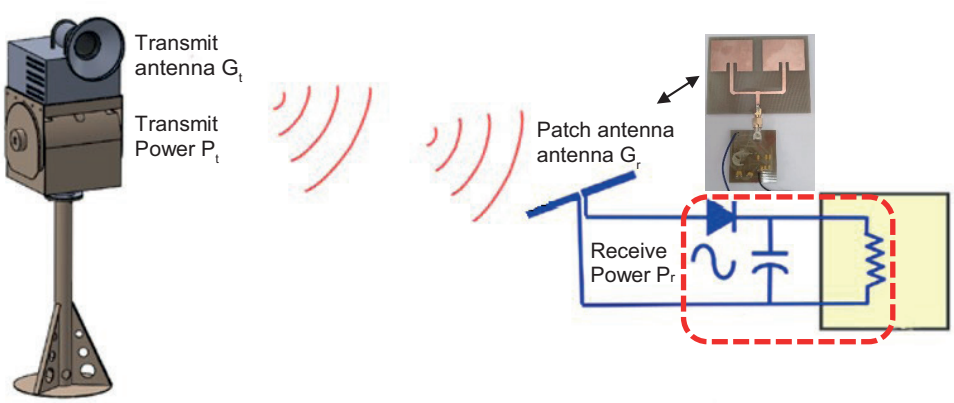

Figure 4. Diagram of transmitting antenna and receiving antenna.

Where the wavelength

$$\lambda = \frac{C}{f} = \frac{3.10^8}{2.45.10^9} = 0.122\,\text{m} = 12\,\text{cm} \tag{5}$$

Where G_r is the Gain of the patch antenna, and λ is the wavelength at 2.45 GHz. From table 2, the Gain is G = 5.25 dBi. Using Equation (4), the effective area of the dipole antenna is 6.22 $\times 10^{-3}$ m^2. The power density W_i transmitted by the conical horn antenna at distance R can be expressed as

$$W_i = \frac{P_t G_r}{4\pi R^2} = \frac{P_t A_{et}}{\lambda^2 R^2} \tag{6}$$

Where:

P_t is the transmitted power,
A_{et} is the effective area of the conical transmitter horn antenna,
R is the distance between transmitting and receiving antennas.

For the conical horn antenna, the Gain (G) can be expressed as

$$G = (\frac{\pi D_f}{\lambda})^2 A_{er} \tag{7}$$

The aperture efficiency (e_A) can be expressed as

$$A_{er} = \frac{G}{\left(\frac{\pi Df}{\lambda}\right)^2} = \frac{7.22}{\left(\frac{3.14\times 0.27}{0.122}\right)^2} = 0.1495\,\text{m}^2 \tag{8}$$

The effective area of the pin-fed horn antenna is the physical area (A) times the efficiency. The power (P_r) received by the dipole antenna can be expressed as:

$$P_r = W_i A_{er} = \frac{P_t A_{et} A_{er}}{\lambda^2 R^2} \tag{9}$$

Equation (9) shows the power required to transmit versus the distance between the transmitting and receiving antennas to obtain the maximum strength at the receiving point. Assume that distance R lies in the far-field of the conical horn antenna. This Equation describes the received power at close-in (reference) distances [W]

$$P_{rx} = P_{tx} G_{tx} G_{rx} \left(\frac{c}{4\pi D_r f_0}\right)^2 \tag{10}$$

Close-in received power in dBm

$$P_{rx} = 10\log\left(\frac{P_r}{0.001}\right) \tag{11}$$

Close-in received power in dBw

$$P_{rx}(\text{dBW}) = 10\log\left(\frac{P_r}{0.001}\right) \tag{12}$$

Received power calculated using reference power in dBm

$$P_{rx} = P_r(\text{dBm}) + 20\log\left(\frac{d_0}{d}\right) \tag{13}$$

Received power calculated using reference power in dBw

$$P_r(\text{dBW}) = P_r(\text{d0BW}) + 20\log_{10}\left(\frac{d_0}{d}\right) \tag{14}$$

Equation (15) represents the path loss

$$P_L = \frac{P_t}{P_r} \tag{15}$$

According to Equation (10), the reflection-free propagation where the far-field depends on distance as (1/r), while the power density falls off as ($1/r^2$), as shown in Figure 5.

Figure 6 illustrates how the transmitter antenna should be positioned face-to-face with the receiver antenna to enhance energy harvesting from the RF transmitter source. The power density harvested depends on the direction of the receiving and transmitting antennas. We simulated the power received after the RF power transmission was set to 2 kW. Figure 6A illustrates the decrease in received power (W) as the gap distance increases, resulting in poor reception. Figures 6B and 6C show the received power (dBm, dBW) as the distance (m) function. There is no other effect other than the decrease in power due to distance and antenna parameters in the simulation. Antenna parameters are not included in the calculation of free-space path loss, as shown in Figure 6D.

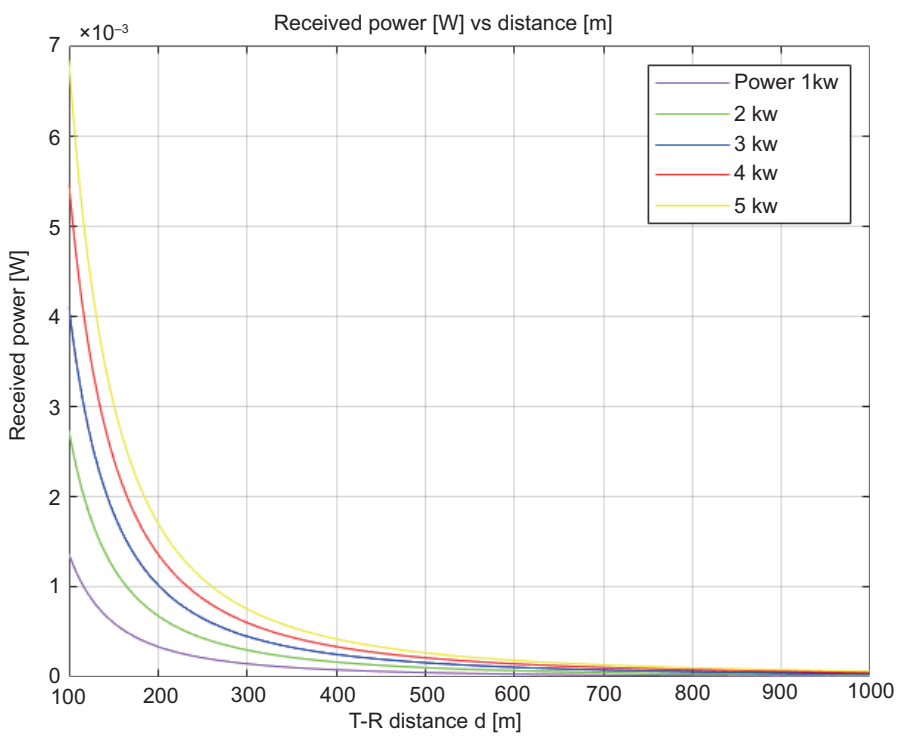

Figure 5. Received power (W) VS distance (m).

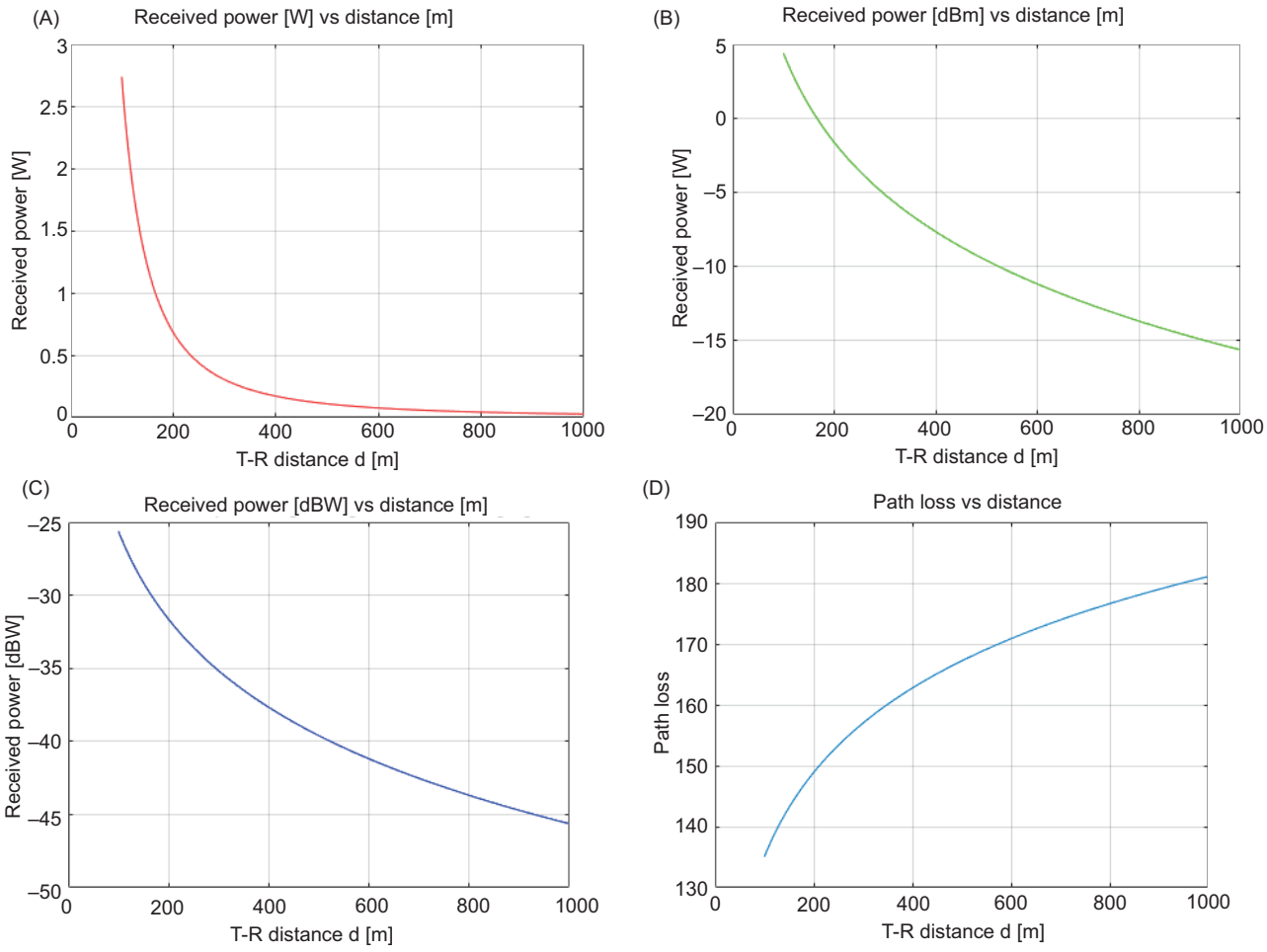

Figure 6. Simulation: (A) Received power (W) vs distance (m), (B) Received power (dBm) vs distance (m), (C) Received power (dBW) vs distance (m), (D) Path loss vs distance.

RF microwave transmitter system

The microwave generator used in this study is an MSAPS (2kW Industrial Microwave Generator (MSPS2000)) (Park and Youii, 2020). As illustrated in Figure 7, these industrial microwave generators consist of a waveguide launcher, power supply, and magnetron in a compact enclosure, resulting in competitive, space-saving add-on generators. To increase the efficiency of RF transmission, we provided a water supply system for cooling.

An antenna should be designed with high Gain and directivity to create a wireless charging device. The CST microwave simulator is used to simulate and optimise transmitter antennas, mainly for microwave radiation and power transmission. The radiation patterns of pin-fed horn antennas were taken into account when determining the maximum gain value, directivity, and area of operation of these antennas. Figure 8 contains a sketch of a pin-fed horn antenna with a linear flare.

The Gain of a horn antenna is:

$$G = \frac{4\pi}{\lambda^2} \int_{ap} W_g H_g \qquad (17)$$

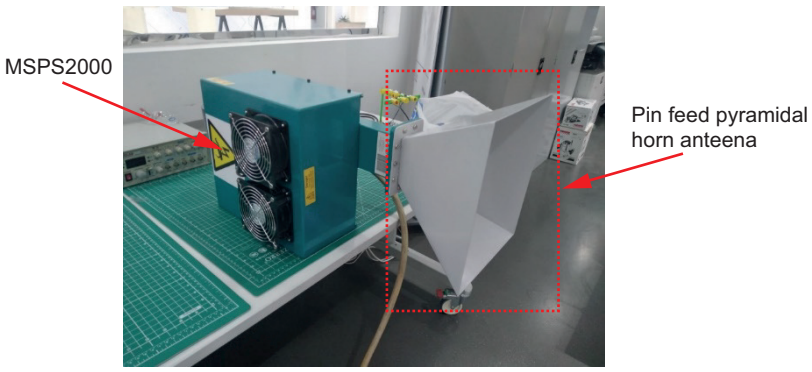

Figure 7. The MSPS2000 Industrial Microwave Generator (2.5kW).

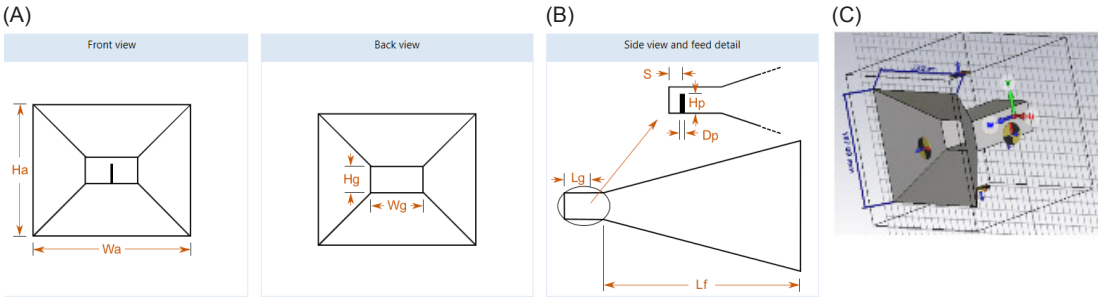

Figure 8. The pin-feed pyramidal horn antenna sketches: (A) Front and back view, (B) Side view, (C) 3D view.

Dimensions of waveguides:

$W_g = 0.8382 \times \lambda = 98.05$ mm (Waveguide width)
$H_g = 0.3925 \times \lambda = 124.91$ mm (Waveguide length)

Where the aperture dimensions are:

$W_a = 258.9$ mm (Aperture width)
$H_a = 187.0$ mm (Aperture height)

The antenna metal thickness is:

$T_s = 0.001 \times$ wavelength centre $= 0.001 \times 124.913$ mm $= 0.1249$ mm

Table 1 contains values derived from the CST microwave software. In the following sections, we discuss and analyse the results.

All physical and electromagnetic properties of the pin-feed pyramidal horn antenna were investigated, including Reflection coefficient, Directivity, Smith Chart, and Radiation pattern 3D. Figure 9A demonstrates that we achieve a perfect return loss of -29.875 dB at 2.45 GHz. The antenna bandwidth is approximately 450 MHz (18.26%) at 2.45 GHz, and the Voltage Standing Wave Ratio (VSWR) is 1.07. Figure 9B shows the directivity gain at 2450 MHz is 12.71 dB. Input impedance is measured using the Smith chart.

Figure 9C illustrates how the antenna impedance varies with operating frequency. Based on the 3-D radiation pattern plots, we conclude that the antenna is highly directive and has a maximum gain of approximately 12.77 dBi, as shown in Figure 9D.

Name	Description	Value
Wg	Waveguide width	98.06 mm
Hg	Waveguide height	49.03 mm
Lg	Waveguide length	124.9 mm
Wa	Aperture width	258.9 mm
Ha	Aperture height	187.0 mm
Lf	Flare length	76.79 mm
Hp	Feed-pin height	28.24 mm
Dp	Feed-pin diameter	1.249 mm
S	Feed-pin inset (distance from the back wall)	23.47 mm
Xx	Device X-dimension	258.9 mm
Y	Device Y-dimension	187.0 mm
Z	Device Z-dimension	201.7 mm

Table 1. Horn antenna parameters.

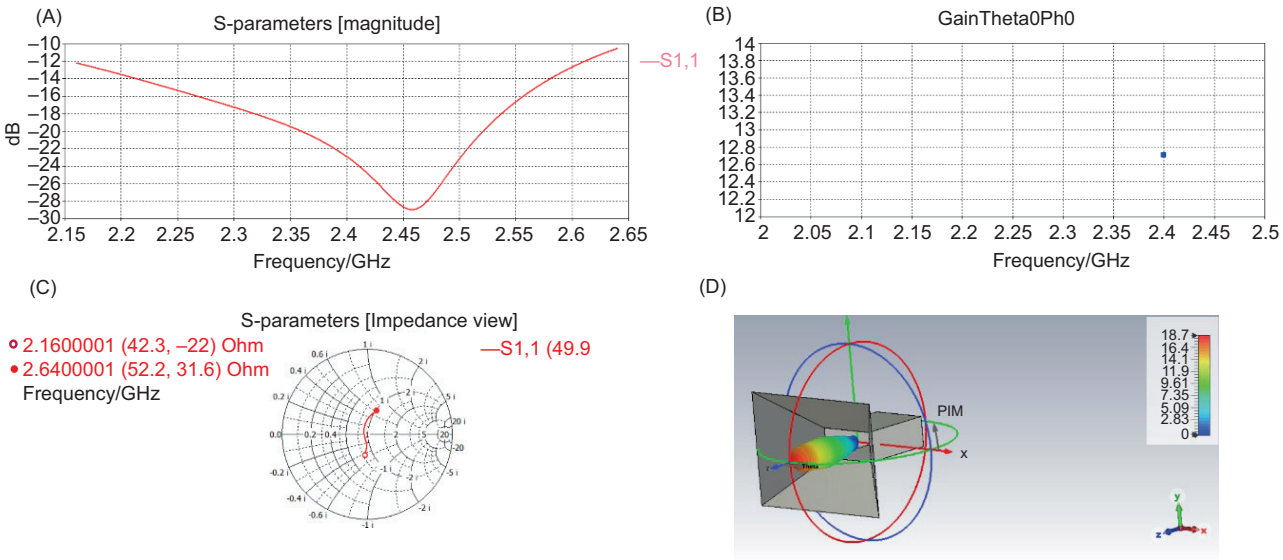

Figure 9. Simulation of pin feed horn antennas: (A) Reflection coefficient of a horn antenna, (B) The directivity Gain of the transmitter, (C) smith chart, 3-D radiation pattern plots (D).

Initially, the geometry of a pyramidal horn antenna with dimensions of the aperture width W_a =258.9 mm, height aperture wall H_a =187.0 mm, the flare length = 76.79 mm; similarly, dimensions of waveguide width W_g =98.05 mm, waveguide length H_g = 124.91 mm, are modelled in Figure 9D.

The phase errors (H-plane)

$$t = \frac{Wa^2}{8\lambda L_1} = 0.1276$$

The phase errors (E-plane)

$$s = \frac{Ha^2}{8\lambda L_2} = 0.0714$$

Figure 10. Prototype constructed.

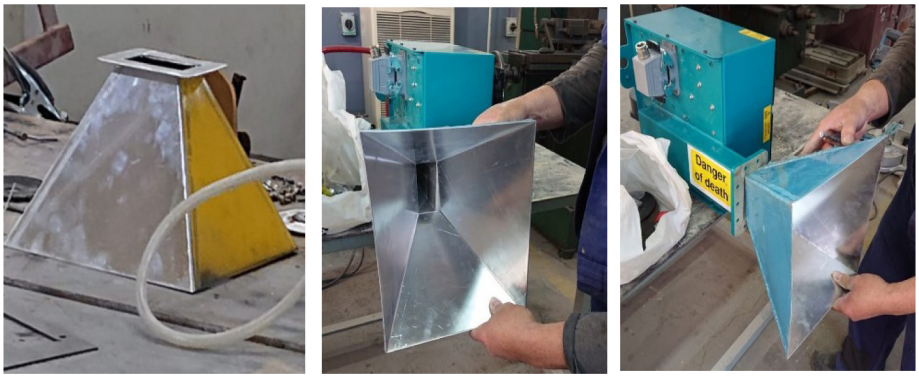

Table 2. Typical characteristics.

Bandwidth	Gain	Size	Impedance	Pattern	Polarization
>20%	12.77	187mm X 259mm	50Ω	Directional	Linear

The phase error (t) in (H-plane) differs from the phase error (s) in (E-plane). Figure 10 contains a photograph of a pin-feed pyramidal horn antenna. The dimensions of pyramidal flared antennas are 187 mm (width) and 259 mm (height), whereas the thickness of the antenna metal is 0.127 mm.

Table 2 has a summary of the distinguishing characteristics of pin-feed pyramidal horn antennas. The antenna's polarisation is linear and directional, and its impedance is 50Ω.

Power harvester system

Embedded wireless power supplies can provide power to military devices for a 36-hour patrol without any contact and reduce battery weight and size. Microwave energy is converted into DC power by the rectifier circuit. As shown in Figure 11, the wearable harvesting system consists of three elements, and this subsection describes each component in detail.

Twin inset-feed patch antenna

Energy harvesters should be small, lightweight, inexpensive, and easily concealed in clothing. The array patch antenna is the optimal choice for this application due to its flexibility and geometry (Eltresy *et al.*, 2018; Li and Hao, 2017). Generally, broadband antennas can operate across various frequencies, especially when incorporated into protective vests. The radiation strength of a patch antenna feed is dependent on its beamwidth. Accordingly, an RF4 substrate with a dielectric height of 1.6 mm was chosen, which provided the essential design parameters.

Figure 11. Wearable RF harvesting device.

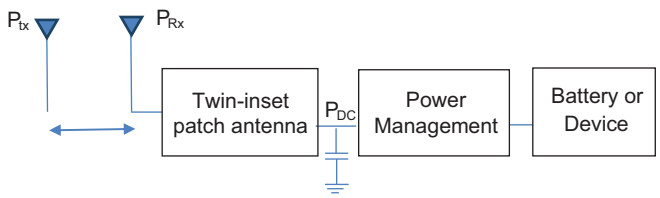

Where:

Speed of light C= 3 x 10^8 m/s
The dielectric constant of the substrate ε_r = 4.4

The schematic of the microstrip patch antenna showing the optimal parameters for Microstrip Line (MLIN), Microstrip Line Open-Circuited Stub (MLOC), Microstrip Curve (MCURVE), and Microstrip Asymmetric Coupled Line (MACLIN) (Ren *et al.*, 2020). It is necessary to add the MACLIN to the design to create the inset feed line, as shown in Figure 12. According to Equation (18), W1 and W3 are equivalent and determined according to the substrate width (W).

$$W1 = W3 = \frac{W - 9}{2} \tag{18}$$

On the other hand, the W2 is equal to the width of the microstrip line feed, s in Equation (18). Moreover, (S1) and (S2) are the gaps of the inset feed, where both were equal to (W_f).

The width of microstrip line feed, (W_f), is computed in Equation (19):

$$W_f = \left\{ \left(\frac{e^H}{8} - \frac{1}{4e^H} \right)^{-1} \right\} \times 1.6\text{mm} \tag{19}$$

Moreover, the length of the microstrip line feed (L_f) is obtained through Equation (20) below:

$$L_f = \theta \frac{\lambda_g}{360^0} \tag{20}$$

Where (λ_g):

$$\lambda_g = \frac{C}{f \times \sqrt{\varepsilon_{reff}}} \tag{21}$$

The following Equation is used to calculate the notch width:

$$g = \frac{c \times 4.65 \times 10^{-12}}{\sqrt{2 \times \varepsilon} \times f_r} \tag{22}$$

In this optimised circuit, with the FR4 dielectric substrate (ε_r = 4.6, tan δ = 0.02, and h = 1.6mm), fr = 2.4 GHz, the relative bandwidth is more significant than 1%. At 2.444 GHz, the proposed patch antenna has a directivity of 7.431 dBi and a gain of 4.518 dBi, as shown in Figures 13 (a) and 13 (c), respectively. With an operating frequency of 2.431 GHz, we obtained an acceptable return loss, S11= -17.167, dB. At 2.45 GHz, the antenna has a standing wave ratio of 1.056 with a bandwidth of approximately 32 MHz.

The different widths of the feed lines result in further distribution of current. At 2.448 GHz, we can see that the antenna and the signal source are almost perfectly matched, with no imaginary parts for impedance. This results in the accurate transmission of all signals.

Where:
Z= (Z_0 × (0.57 + j0.01)).

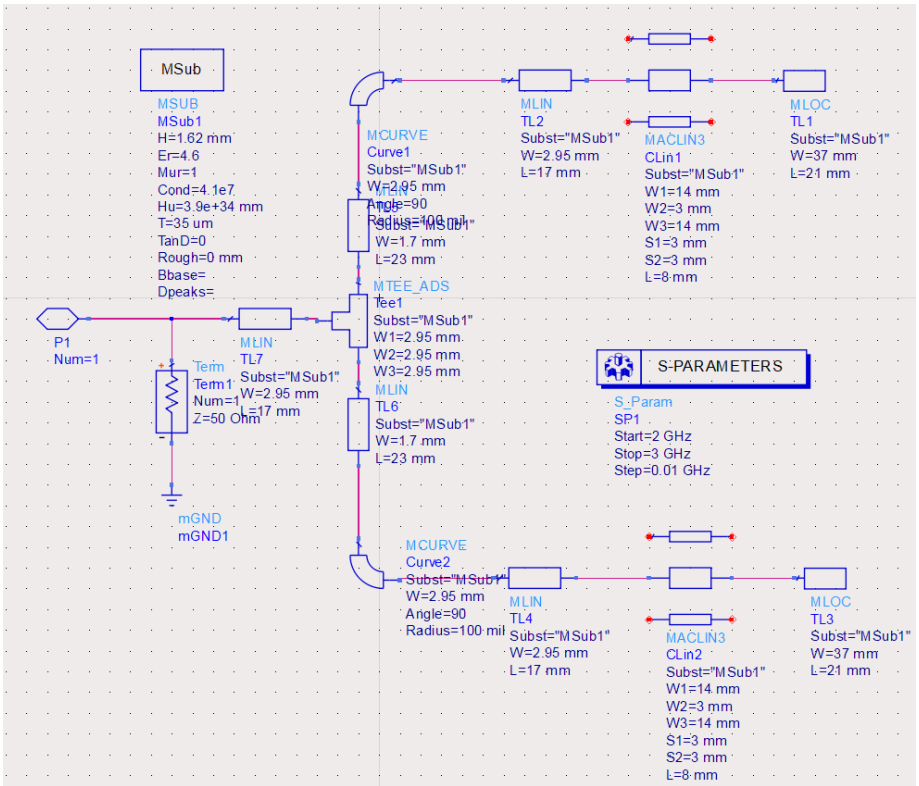

Figure 12. Circuit schematic for twin inset-feed patch antennas.

This antenna performs acceptably for harvesting RF energy. The next step will be to examine the circuit design for rectifier harvesters.

Rectifier Investigation

This section describes the fabrication of RF rectifiers, starting with selecting components according to the desired output voltage and output current and analysing the performance of the RF rectifier harvesting circuit based on high-frequency diode components (Akter *et al.*, 2014; Ali *et al.*, 2016; Chaari and Al-maadeed, 2020; Matsunaga *et al.*, 2015; Pinto *et al.*, 2021). The output voltage (V_{out}) achieved is given by this variation in (RL) value, as present in Equation (23):

$$V_{out} = V0\left(\frac{1}{\frac{R_0}{R_L}+\frac{1}{n}}\right) \tag{23}$$

As shown in Figure 14, a Schottky diode named HSMS2810 is used as part of the RF energy harvesting circuit. In this experiment, the voltage gain decreased as the number of steps increased, whereas a higher voltage is obtained by increasing the number of steps.

As shown in Figure 15, the DC output voltages obtained from the simulation of a five-stage voltage multiplier are 7.031V when using HSMS2700 diodes. We simulate a five-stage voltage multiplier using different Schottky diodes until we reach the high output voltage (HSMS2800, HSMS2850, HSMS2860, HSMS2810, HSMS810, HSMS2700,

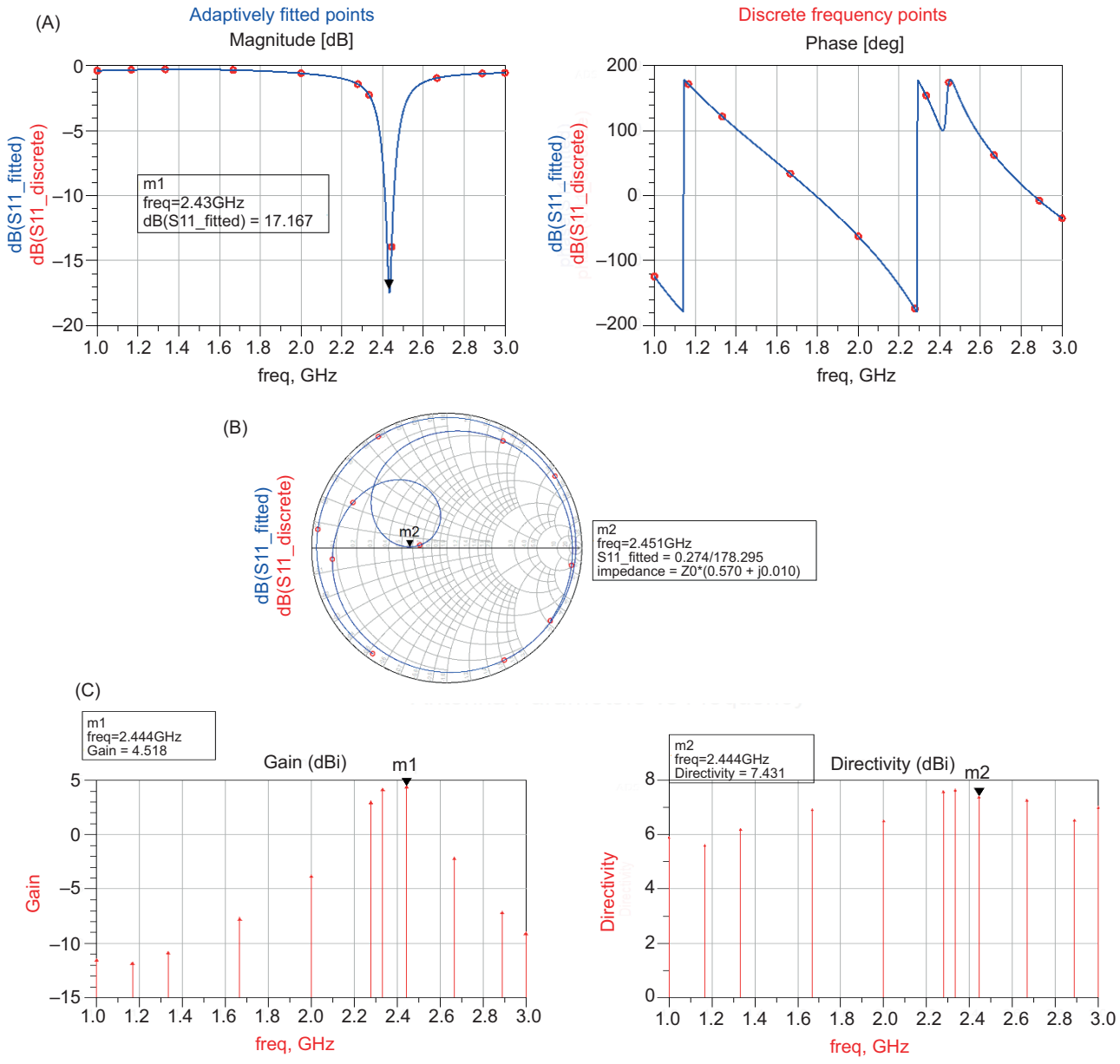

Figure 13. Tin inset-feed patch antenna simulation: (A) S11 performance, (B) Current simulation, (C) Antenna Smith chart, (D) Gain and directivity of the proposed antenna.

HSMS270B). According to Table 3, the HSMS-281X family has a high output voltage due to low flicker noise.

It has a low series resistance, low forward voltage at current levels, and good RF characteristics, making it an excellent choice for RF scavenging. The HSMS-285x detector diodes, as shown in Table 3, are zero-bias detectors designed for applications that involve small signals below 1.45 GHz. Schottky diodes HSMS-2850, despite their apparent high series resistance, provide low power levels in all the above RF rectifier topologies.

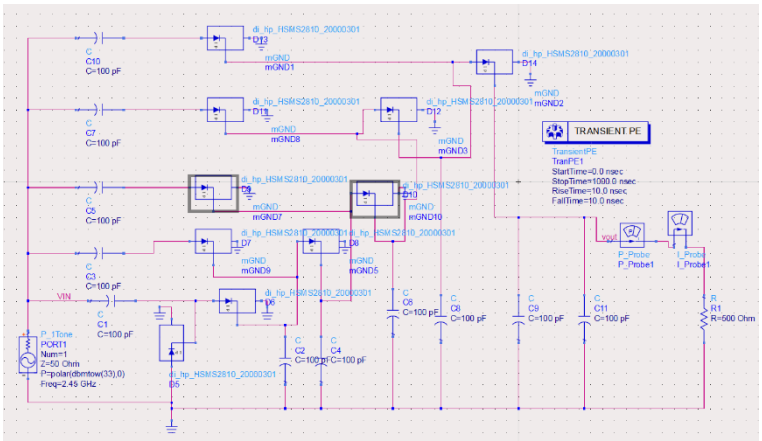

Figure 14. Circuit design for RF harvesting utilising a five-stage voltage multiplier with the diode HSMS-2810 (Agilent ADS).

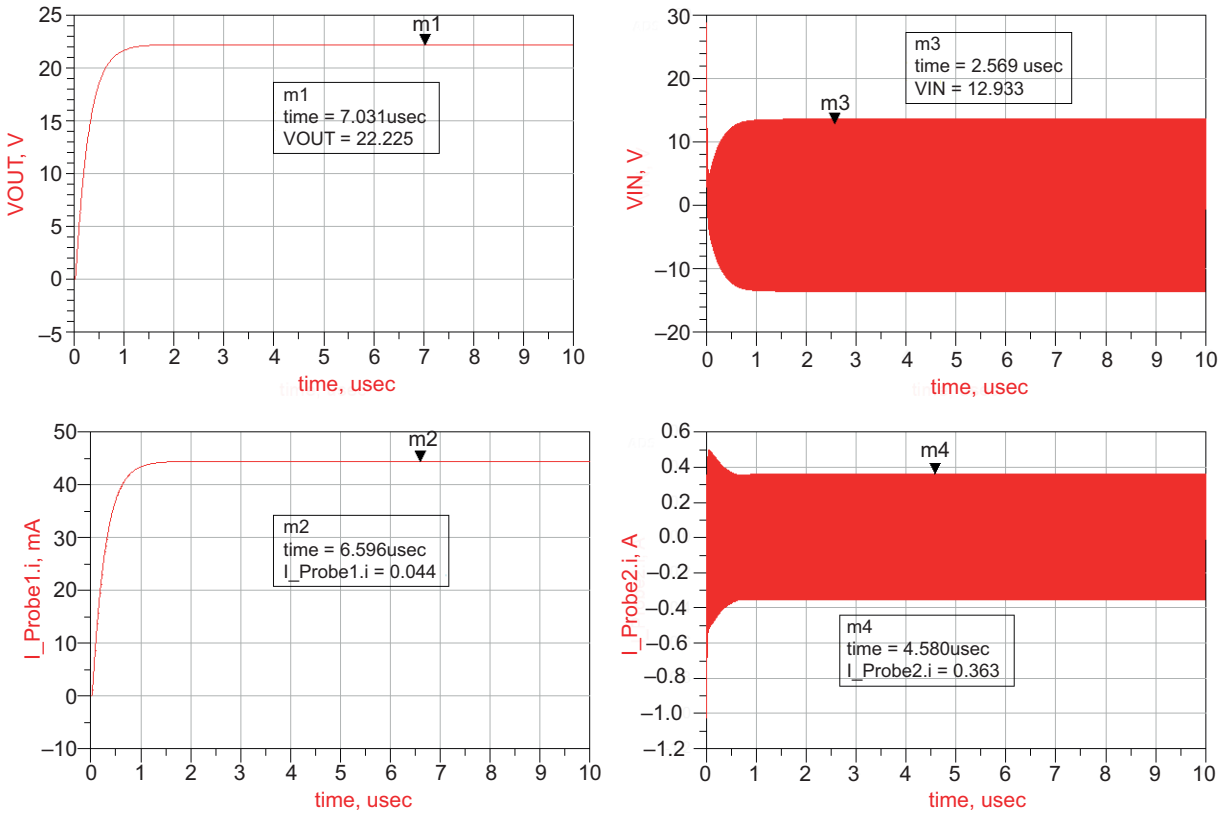

Figure 15. The simulation results after optimization (HSMS2700).

HSMS 8101 is approximately 3.1 times more efficient than HSMS 2850, as shown in Figure 16. In this test, HSMS 2810 provides high output voltage.

Prototype result and discussion

The portable microwave radiation station features a power output range of 100W to 2kW and operates at a frequency of 2.45GHz. Wireless energy calculators use equations to estimate the amount of microwave energy present at the receiver and the level of

Diode	P_{in} (dB)	Load resistance (Ω)	V_{out} (v)	I_{out} (mA)	P_{out} (w)	Efficiency $\eta = \frac{V_{out} \times I_{out}}{P_{in}}$ (%)
HSMS2800	33	500 Ω	9.75	20	0.19	5.91
HSMS2850			2.00	4.12	0.0081	0.25
HSMS2860			3.86	8	0.03	0.93
HSMS2810			11.60	23	0.27	8.09
HSMS8101			6.64	13	0.088	2.61
HSMS2700			7.18	14.2	0.103	3.09
HSMS270B			0.24	0.52	$1.06e^{-4}$	0.003

Table 3. Schottky diode HSMS-2800, HSMS-2850, HSMS-2860, HSMS-2810, HSMS8101, HSMS2700, and HSMS-270B efficiency comparison.

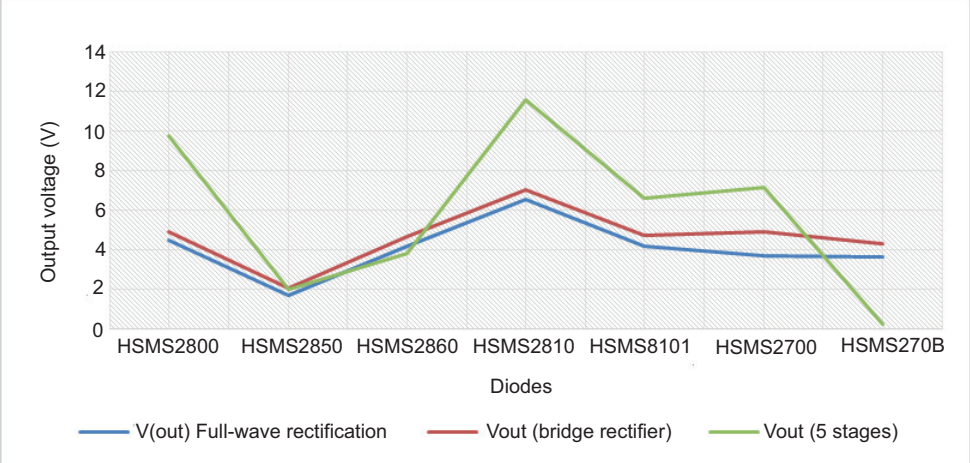

Figure 16. The output DC voltage among Schottky diode HSMS-2800, HSMS-2850, HSMS-2860, HSMS-2810, HSMS8101, HSMS2700, and HSMS-270B.

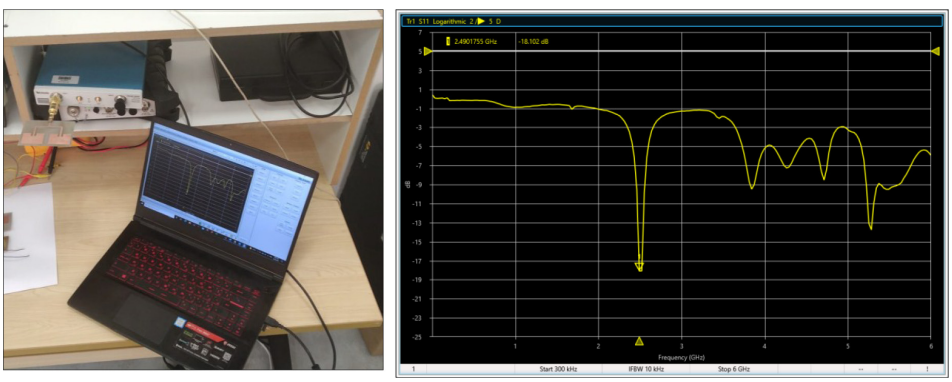

Figure 17. Setup for measuring antenna parameters.

RF power converted to DC outputs, assuming a direct line of sight between the patch antenna and the horn antenna. We entered the gain values of the (Tx) and (Rx) antennas into the wireless power calculator. To measure the S11 of the fabricated antenna, we used a vector network analyser (VNA) TTR506A. As shown in Figure 17, the estimated S11 value is -18.102 dBi, while the theoretical simulation value is -17.167 dBi. Accordingly, this antenna matches much better at 2.45 GHz, with a smaller reflection. A receiver antenna's maximum Gain is 4.510 dB. (TX) antenna prototypes have been constructed and measured using the Vector Network Analyser to determine the S_{11}. S_{11} was estimated to be -26.13 dBi instead of -28.16 dBi as predicted. The receiver antenna can achieve a gain of 12.510 dB. Using a patch antenna and HSMS-2810, the rectenna generates

a maximum DC voltage of 11.7 V, with an efficiency of 18.75 percent, at an RF power of 20 W.

The line of sight (LOS) between the antennas is one metre to five metres for outdoor testing.

According to Table 4, the strength of the RF power varies with the distance between the microwave power station Pin = 100 W and the receiver circuit. It appears that the harvested power varies significantly with distance.

As a transmitter source, we fixed the RF power at 100 Watts. The rectifying circuit is connected to the twin inset-feed patch antenna using the SMS connector. Figure 18 shows how the bulbs are powered wirelessly.

Conclusion and perspectives

Using an RF energy harvesting device, this project investigated the possibility of generating electricity from the ISM-band to charge many devices on the battlefield. This device can integrate into a protective vest in the future. During a real test, the receiver patch antenna had a reflection coefficient of -32.34 dB and a gain of 15.11 dB. The harvester antenna meets all the specifications required for this application. It produces a high output DC voltage and provides excellent conversion to electricity. At five metres, we achieved 13 watts. In this study, we discovered that wireless power technology could reduce the weight a soldier carries and that soldiers could wirelessly charge all their electronic devices. The effects of this technology on the body of a soldier are not of concern to us, and it is extremely critical to keep it alive and in contact with the command centre. We will change the topology of the rectifier circuit in the next step and check the harvesting circuit's efficiency.

Table 4. Energy harvesting range/ distance.

RF Power transmitting (P_r)	There is a gap between the RF transmitter and the observation point	Harvested energy
100 W	1 metre	26.22 W
	2 metres	19.56 W
	3 metres	14.56 W
	4 metres	14.62 W
	5 metres	10.03 W

Figure 18. Photograph of the RF energy harvesting test setup.

Funding

This research received no external funding.

Author Contributions

Conceptualization, M.Z.C., Validation, M.Z.C., Investigation, M.Z.C., Data curation, O.A., Project administration, R.A. All authors read and agreed to the published version of the manuscript.

Data Availability Statement

Data available in a publicly accessible repository.

Disclosure statement

No potential conflict of interest was reported by the authors.

The authors have obtained copyright permission for the images published in the paper.

References

Akter, N., Hossain, B., Humayun Kabir, M., Bhuiyan, A.H., Yeasmin, M., and Sultana, S. (2014) 'Design and performance analysis of 10-stage voltage doublers RF energy harvesting circuit for wireless sensor network', *Journal of Communications Engineering and Networks*, pp. 84–91. doi: 10.18005/JCEN0202004.

Ali, E.M., Yahaya, N.Z., Perumal, N. and Zakariya, M.A. (2016) 'Development of Cockcroft-Walton voltage multiplier for RF energy harvesting applications', *Journal of Scientific Research and Development*, 3, pp. 47–51, 201.

Beckhusen, R. (2012) 'Army plan: wirelessly recharge gadgets … from 50 feet away', *Wired*, 12 June. Available at: https://www.wired.com/2012/06/wireless-power/ (Accessed: 24 March 2022).

Brewster, R. (2020) *The SCR-536 handie-talkie was the modern walkie-talkie's finicky ancestor*, IEEE Spectrum. Available at: https://spectrum.ieee.org/the-scr536-handietalkie-was-the-modern-walkietalkies-finicky-ancestor (Accessed: 24 March 2022).

Chaari, M.Z. and Al-maadeed, S. (2020) 'Wireless power transmission for the internet of things (IoT)', in *2020 IEEE International Conference on Informatics, IoT, and Enabling Technologies (ICIoT)*. Doha, Qatar: IEEE, pp. 549–554. doi: 10.1109/ICIoT48696.2020.9089547.

Chaari, M.Z. and Al-Rahimi, R. (2021a) 'Energized IoT devices through RF wireless power transfer', in *2021 International Symposium on Electrical and Electronics Engineering (ISEE)*. Ho Chi Minh, Vietnam: IEEE, pp. 199–203. doi: 10.1109/ISEE51682.2021.9418741.

Chaari, M.Z. and Al-Rahimi, R. (2021b) 'The impact of wireless power charging on the future of the battlefield', in *2021 International Wireless Communications and Mobile Computing (IWCMC)*. Harbin City, China: IEEE, pp. 1563–1568. doi: 10.1109/IWCMC51323.2021.9498775.

Chaari, M.Z. and Rahimi, R. (2017) 'Light LED directly lit up by the wireless power transfer technology', in *2017 International Conference on Radar, Antenna, Microwave, Electronics, and Telecommunications (ICRAMET)*. Jakarta: IEEE, pp. 137–141. doi: 10.1109/ICRAMET.2017.8253162.

Collins, J.J. (2015) *Chapter 1 | Initial planning and execution in Afghanistan and Iraq*. Washington, DC: National Defense University Press. Available at: https://ndupress.ndu.edu/Media/News/News-Article-View/Article/915829/chapter-1-initial-planning-and-execution-in-afghanistan-and-iraq/ (Accessed: 24 March 2022).

Eltresy, N.A. Dalia N. Elsheakh, Esmat Abdallah, and Hadia M. El-Hennawy. (2018) 'Tri-band antenna for energizing IoT low power devices', in *2018 IEEE Global Conference on Internet of Things (GCIoT)*. Alexandria, Egypt: IEEE, pp. 1–5. doi: 10.1109/GCIoT.2018.8620145.

Harper, J. (2015) 'The army wants to power up dismounted soldiers', *National Defense*, 100(743), pp. 42–42. Available at: https://www.jstor.org/stable/27021024 (Accessed: 15 October 2015).

Ishibashi, K., Ida, J., Nguyen, L.T., Ishikawa, R., Satoh, Y., and Luong, D.M. (2019) 'RF characteristics of rectifier devices for ambient RF energy harvesting', in *2019 International Symposium on Electronics and Smart Devices (ISESD)*. Badung-Bali, Indonesia: IEEE, pp. 1–4. doi: 10.1109/ISESD.2019.8909660.

Lafontaine, D. (2019) *Army boosts soldier battery power for greater lethality, mobility*. Available at: https://www.army.mil/article/224879/army_boosts_soldier_battery_power_for_greater_lethality_mobility (Accessed: 24 March 2022).

Li, Y. and Hao, Z.-C. (2017) 'A wideband switched beam antenna for full 360 coverage', in *2017 Sixth Asia-Pacific Conference on Antennas and Propagation (APCAP)*. Xi'an: IEEE, pp. 1–3. doi: 10.1109/APCAP.2017.8420905.

Liu, J., Zhao, Z., Ji, J. and Hu, M. (2020) 'Research and application of wireless sensor network technology in power transmission and distribution system', *Intelligent and Converged Networks*, 1(2), pp. 199–220. doi: 10.23919/ICN.2020.0016.

Matsunaga, T., Nishiyama, E. and Toyoda, I. (2015) '5.8-GHz stacked differential rectenna suitable for large-scale rectenna arrays with DC connection', *IEEE Transactions on Antennas and Propagation*, 63(12), pp. 5944–5949. doi: 10.1109/TAP.2015.2491319.

Miller, S.W. (2020) 'More power to your elbow', *Armada International*, 9 June. Available at: https://armadainternational.com/2020/06/more-power-to-your-elbow/ (Accessed: 14 February 2022).

Niesel, J. (2019) 'SCR-300 WW2 radio backpack: the "walkie talkie" that shaped the war', *Warfare History Network*, 27 January. Available at: https://warfarehistorynetwork.com/2019/01/26/scr-300-ww2-radio-backppack-the-walkie-talkie-that-shaped-the-war/ (Accessed: 24 March 2022).

Park, Y. and Youii, D. (2020) 'kW-class wireless power transmission based on microwave beam', in *2020 IEEE Wireless Power Transfer Conference (WPTC)*. Seoul, Korea (South): IEEE, pp. 5–8. doi: 10.1109/WPTC48563.2020.9295626.

Pinto, D., Arun, A., Lenka, S., Colaco, L., Khanolkar, S., Betgeri, S., and Naik, A. (2021) 'Design and performance evaluation of a wi-fi energy harvester for energizing low power devices', in *2021 IEEE Region 10 Symposium (TENSYMP)*. Jeju, Republic of Korea: IEEE, pp. 1–8. doi: 10.1109/TENSYMP52854.2021.9551001.

Ren, R., Huang, J. and Sun, H. (2020) 'Investigation of rectenna's bandwidth for RF energy harvesting', in *2020 IEEE MTT-S International Microwave Workshop Series on Advanced Materials and Processes for RF and THz Applications (IMWS-AMP)*. Suzhou, China: IEEE, pp. 1–2. doi: 10.1109/IMWS-AMP49156.2020.9199653.

Sidhu, R.K., Singh Ubhi, J. and Aggarwal, A. (2019) 'A survey study of different RF energy sources for RF energy harvesting', in *2019 International Conference on Automation, Computational and Technology Management (ICACTM)*. London, United Kingdom: IEEE, pp. 530–533. doi: 10.1109/ICACTM.2019.8776726.

Sigler, D. (2011) *Putting sugar in your tank › Sustainable skies.* Available at: https://sustainableskies.org/putting-sugar-in-your-tank/ (Accessed: 14 February 2022).

Thales (2016) *Reducing the battery burden on the dismounted soldier*, Thales Group. Available at: https://www.thalesgroup.com/en/global/presence/europe/united-kingdom/defence/land-systems/soldier-systems/squadnet/reducing-battery (Accessed: 24 March 2022).

Tran, L.-G., Cha, H.-K. and Park, W.-T. (2017) 'RF power harvesting: a review on designing methodologies and applications', *Micro and Nano Systems Letters*, 5(1), p. 14. doi: 10.1186/s40486-017-0051-0.